The Bradykinin B2 Receptor Gene Is a Target of Angiotensin II Type 1 Receptor Signaling

Bing Shen,*† Lisa M. Harrison-Bernard,‡ Andrew J. Fuller,† Vanessa Vanderpool,* Zubaida Saifudeen,* and Samir S. El-Dahr*

*Department of Pediatrics, Section of Pediatric Nephrology, †Department of Physiology, Tulane University Health Sciences Center, and ‡Department of Physiology, Louisiana State University Health Sciences Center, New Orleans, Louisiana

Cross-talk between G protein–coupled receptors (GPCR) is known to occur at multiple levels, including receptor heterodimerization and intracellular signaling. This study tested the hypothesis that GPCR cross-talk occurs at the transcriptional level. It was demonstrated that the bradykinin B2 receptor gene (*BdkrB2*) is a direct transcriptional target of the angiotensin II (AngII) type 1 receptor (AT_1R) in collecting duct cells. AngII induced *BdkrB2* mRNA expression in mouse inner medullary collecting duct cells, and this effect was abrogated by AT_1R blockade; in contrast, AT_2R blockade was ineffective. Actinomycin D, an inhibitor of gene transcription, abrogated AngII-stimulated *BdkrB2* expression. In addition, AngII produced dosage- and time-dependent increases in B2 receptor protein levels (2.9 ± 0.4 fold; $P < 0.05$). AngII stimulated phosphorylation of cAMP response element binding protein (CREB) on Ser-133 and assembly of p-CREB on the *BdkrB2* promoter *in vivo*. Moreover, AngII induced hyperacetylation of *BdkrB2* promoter–associated H4 histones, a chromatin modification that is associated with gene activation. Mutations of the CRE abrogated AngII-induced activation of the *BdkrB2* promoter. AngII-treated inner medullary collecting duct cells exhibited augmented intracellular calcium signaling in response to bradykinin, confirming the functional relevance of AT_1-B2 receptor signaling. Finally, studies that were conducted in angiotensin type 1 receptor (*Agtr1*)-null mice revealed that *BdkrB2* mRNA levels were significantly lower in the renal medulla of $Agtr1_A^{-/-}$ and $Agtr1_{A/B}^{-/-}$ than in $Agtr1^{+/+}$ and $Agtr1_B^{-/-}$ mice. It is concluded that *BdkrB2* is a downstream target of the AT_1R-CREB signaling pathway. Transcriptional regulation represents a novel form of cross-talk between GPCR that link the renin-angiotensin and kallikrein-kinin systems.

J Am Soc Nephrol 18: 1140–1149, 2007. doi: 10.1681/ASN.2006101127

The kallikrein-kinin and renin-angiotensin systems (KKS and RAS, respectively) are key regulators of cardiovascular and renal homeostasis. The balance between these two systems affects salt sensitivity, blood volume, vascular reactivity, and growth and development (reviewed in references [1–3]). The most widely recognized cross-talk between the KKS and RAS is at the level of the angiotensin-converting enzyme. More recently, physical and functional interactions between the receptors for angiotensin II (AngII) (AT_1R) and bradykinin (B2R) have been reported, adding another layer of cross-talk between the RAS-KKS cascades. AT_1R and B2R form heterodimers in cultured cells and intact tissues, and the receptor complex signals as a "super" AT_{1A} receptor (4,5). Infusion of subpressor dosages of AngII upregulates cardiac myocyte *BdkrB2* gene expression in mice (6). Furthermore, treatment of vascular smooth muscle cells in culture with AngII produces a time-dependent induction of *BdkrB2* mRNA, an effect that is inhibited by AT_1R blockade (7). However, the mechanisms whereby AngII regulates *BdkrB2* gene expression are not fully understood, and whether AT_1R–B2R cross-talk operates in other AngII target tissues, such as the kidney, is not entirely clear.

We previously demonstrated that the *BdkrB2* promoter is regulated by a highly conserved *cis*-acting module that represents the binding sites for the transcription factors p53 and cAMP response element binding protein (CREB), located at nucleotide positions −44 to −69 relative to the transcription start site (8–10). The *BdkrB2* modular enhancer drives reporter expression in mouse renal inner medullary collecting duct (IMCD3) cells but is considerably weaker in other cell types (10). Upon activation, CREB is phosphorylated on Serine 133 (p-CREB), a modification that facilitates recruitment of a co-activator, CREB-binding protein (CBP/p300) (11,12). In addition to bridging CREB with the basal transcription machinery, CBP/p300 acetylates promoter-associated histones (13), relaxes local chromatin structure, and allows better access of transcription factors to the cis-regulatory elements (14). It has also been shown that p-CREB interacts with and recruits p53 to target promoters that contain composite target sites (15). Given that AngII stimulates the phosphorylation of p53 (on serine 15) (16,17) and CREB (on serine 133) (18), we hypothesized that

Received October 18, 2006. Accepted January 25, 2007.

Published online ahead of print. Publication date available at www.jasn.org.

Address correspondence to: Dr. Samir S. El-Dahr, Department of Pediatrics, SL-37, Tulane University Health Sciences Center, 1430 Tulane Avenue, New Orleans, LA 70112. Phone: 504-988-377; Fax: 504-988-1852; E-mail: seldahr@tulane.edu

 ISSN: 1046-6673/1804-1140

AngII signaling converges on the p53-CRE enhancer to stimulate *BdkrB2* gene transcription. Our results indicate that AT_1R signaling activates CREB phosphorylation and *in vivo* assembly of p-CREB on the *BdkrB2* promoter in conjunction with histone hyperacetylation. AngII stimulates *BdkrB2* gene transcription in IMCD3 cells *via* the AT_1R. Studies in genetically targeted mice demonstrated that control of *BdkrB2* gene by AngII occurs in the renal medulla and is mediated *via* the AT_1R subtype A (AT_{1A}) rather than AT_{1B}. Thus, under conditions of augmented AngII and AT_1R signaling, B2R expression will be enhanced, thereby maintaining a balance of these two powerful counterregulatory systems.

Materials and Methods

Animals and Tissues

The animal study protocol was performed in accordance with the National Institutes of Health Guide for the Care and Use of Laboratory Animals and approved by the Institutional Animal Care and Use Committee of Tulane University and Louisiana State University. Tissues were harvested from adult male wild-type, $Agtr_{1A}{}^{-/-}$, $Agtr_{1B}{}^{-/-}$, and $Agtr_{1A/B}{}^{-/-}$ mice (3 mo of age; $n = 3$ each). Details of breeding and genotyping were previously published (19). Total RNA was extracted from the heart, kidney medulla, and kidney cortex using the Trizol reagent (Invitrogen, Carlsbad, CA). Total RNA from mouse embryonic kidneys (E13.5 d) was extracted with RNAqueous-4PCR Kit (Ambion, Austin, TX).

Cell Culture

IMCD3 cells (20) were obtained from American Type Culture Collection (Rockville, MD) and maintained in DMEM/F-12 that contained 10% FBS (Invitrogen) at 37°C in a humidified incubator with 5% CO_2. The cells were plated in duplicate in six-well plates at 2 to 3 $\times$ 10^5 cells/well 2 d before AngII treatment. For avoidance of the confounding effects of growth factors that were present in the serum on B2R expression, IMCD3 cells were grown in serum-free medium for 24 h before treatment. Icatibant (a specific B2R antagonist, 10^{-6} M) and candesartan (a specific AT1 receptor antagonist, 10^{-6} M) were chosen on the basis of their ability to inhibit the hemodynamic and growth-related effects of exogenously infused intravenous BK or AngII (21–25).

Immunofluorescence Staining

IMCD3 cells were cultured on chamber slides to 40 to 50% confluence, washed once with ice-cold 1× PBS, and fixed in ice-cold 4% paraformaldehyde/0.1% glutaraldehyde solution at room temperature for 10 min. After removal of the fixatives, cells were permeabilized with ice-cold PBS that contained 1% Triton X-100 for 15 min at room temperature and blocked with ice-cold PBS that contained 1% BSA for 10 min. Cells were incubated with a polyclonal rabbit B2R antibody (AS276-283, diluted 1:500, from Dr. Muller-Esterl, Mainz, Germany) (26) overnight at 4°C followed by extensive washes with PBS that contained 1% BSA. The cells were subsequently incubated with secondary antibody (Alexa Fluor 594; Molecular Probes, Eugene, OR; 1:200) for 2 h at room temperature and subjected to extensive washes thereafter. Cells were then incubated with the AT_1R antibody (sc-1173; Santa Cruz Biotechnology, Santa Cruz, CA; 1:200) (27) overnight at 4°C followed by extensive washes with PBS that contained 1% BSA. Subsequently, the cells were incubated with secondary antibody (Alexa Fluor 488; Molecular Probes; 1:2000) for 2 h at room temperature. After extensive washes, the sections were covered with fluorescence mounting medium that contained a nuclear stain, DAPI. Immunofluorescence images were obtained with an Olympus BX51TRF microscope and an integrated Magnafire SP Digital "Firewire" Camera System (Olympus American Inc., Center Valley, PA). Negative controls included cells that were incubated in the absence of primary antibodies (single or both).

Western Blot Analysis

Immunoblotting was performed as described previously (10). Primary antibodies were a polyclonal anti-B2R (diluted 1:1500), CREB (Cell Signaling, Danvers, MA; 48H2, 9197; 1:1000), and p-CREB (Upstate Biotechnology, Lake Placid, NY; 06-519; 1:500). After three washes in PBS/Tween, the nitrocellulose membrane was exposed for 1 h at room temperature to the secondary antibody (horseradish peroxidase–linked goat anti-rabbit IgG). Immunoreactive bands were visualized using the ECL detection system (Amersham, Piscataway, NJ). The immunoblots were exposed to Hyperfilm-ECL films. The blots were then reprobed with a β-actin antibody (Sigma, St. Louis, MO; 1:4000) as a loading control.

Reverse Transcriptase–PCR

After DNAse I digestion, 2 to 3 μg of total RNA was reverse-transcribed using SuperScript II Reverse Transcriptase (Invitrogen) in a 22-μl volume. One to three microliters of the reaction volume was used in a PCR volume of 25 μl. The primer sequences for *BdkrB2* were as follows: Upstream 5′-AGA ACC TCT TTG TCC TCA GCG-3′; downstream 5′-CGT CTG GAC CTC CTT GAA CT-3′. PCR was performed at 94°C for 50 s, 60°C for 60 s, and 72°C for 90 s, 1.0 mM $MgCl_2$, 30 cycles. The product size was 572 bp. The primer sequences for $Agtr1_A$ were as follows: Upstream 5′-GCA TCA TCT TTG TGG TGG G-3′; downstream 5′-GAA GAA AAG CAC AAT CGC C-3′. PCR was performed at 94°C for 1 min, 55°C for 1 min, and 72°C for 2 min, 2.0 mM $MgCl_2$, 35 cycles. The product size was 641 bp. The primer sequences for *Agtr2* were as follows: Upstream 5′-AGT GCA TGC GGG AGC TG-3′; downstream 5′-GAC AAC AAA ACA GTG AG-3′. PCR was performed at 94°C for 1 min, 53°C for 1 min, and 72°C for 2 min, 1.5 mM $MgCl_2$, 35 cycles. The product size was 309 bp. The primer sequences for glyceraldehyde-3-phosphate dehydrogenase (GAPDH) were as follows: Upstream 5′-CCC CTG GCC AAG GTC ATC CAT GAC AAC TTT-3′; downstream 5′-GGC CAT GAG GTC CAC CAC CCT GTT GCT GTA-3′. PCR was performed at 94°C for 50 s, 55°C for 50 s, and 72°C for 90 s, 1.5 mM $MgCl_2$, 27 cycles. The product size was 516 bp. PCR reactions were visualized on a 1% agarose gel, and densitometric analysis was performed with the ChemiImager 4400 program (Alpha Innotech, San Leandro, CA).

Intracellular Calcium Measurements

Peak increases in $[Ca^{2+}]_i$ after activation of B2R in IMCD3 cells were evaluated using fluorescence microscopy. IMCD3 cells that were maintained in DMEM/F-12 medium that contained 10% FBS were plated on coverslips in 5-cm-diameter cell culture dishes, mounted in 200-μl perfusion chambers (Warner Instruments, Eugene, OR), and examined using a Nikon Diaphot (Melville, NY) inverted microscope with an attached Photon Technology International (Birmingham, NJ) deltascan fluorescence-based spectrophotometry system with excitation wavelengths set at 340 and 380 nm and emission collected at 510 nm. Cells were continually superfused with PBS that contained 1.8 mM Ca^{2+} at 37°C. Five fluorescence measurements per second were taken with appropriate background elimination. Fluorescence experiments were calibrated *in vitro* using the methods described by Grynkiewicz *et al.* (28).

For testing the effect of AngII on B2R-induced $[Ca^{2+}]_i$ signaling, cells that were plated on coverslips were changed to serum-free medium for

24 h and treated with 10^{-7} M AngII for the subsequent 24 h. Calcium fluorescence was measured in cells that were exposed to PBS for 0 to 100 s, followed by 10^{-7} M bradykinin (BK; 400 s) before being returned to PBS. Untreated cells were used as control. For evaluation of the effect of icatibant (formerly known as HOE-140), a selective B2R antagonist, on AngII-stimulated B2R signaling, calcium fluorescence was measured in AngII-treated cells (×24 h) that were exposed to icatibant (10^{-6} M) for 100 s, followed by exposure to 10^{-7} M BK in the continued presence of icatibant (300 s) before being returned to PBS. Fluorescence intensity measurements were converted to calcium concentrations on the basis of calibration procedures that were previously described (29). Baseline $[Ca^{2+}]_i$ was calculated by taking the average value of the 5-s period before addition of BK to the chamber. Peak change in $[Ca^{2+}]_i$ in response to BK was determined as the peak value of $[Ca^{2+}]_i$ reached on addition of BK minus the baseline. Mean values ± SE are presented for the peak time point value.

Promoter Constructs, Transient Transfection, and Reporter Assays

The *BdkrB2* −94/+55-CAT promoter-reporter construct was previously described (8,9). The mutant *BdkrB2* −94(P1mut)/CAT, −94(CREmut)/CAT, −94(P1mutCREmut)/CAT constructs were generated by introducing point mutations in the −94/+55-CAT construct at the p53-binding site (P1) and CREB binding site (CRE), singly or in combination, using the QuickChange site-directed mutagenesis system (Stratagene, La Jolla, CA) (10). All constructs were subjected to DNA sequencing to verify the sequence and orientation.

IMCD3 cells that were maintained in DMEM/F-12 medium that contained 10% FBS were plated in duplicate in 3.5-cm-diameter six-well plates at 2.0×10^5 cells/well 2 d before transfection, followed by 24 h of serum-free medium 1 d before transfection. Cells that were grown to 80% confluence were transfected with 1 μg of DNA per well of each promoter-reporter construct. One microgram of DNA per well pCAT3 Basic vector (empty vector) was transfected as a control. A β-galactosidase vector, pSVZ (0.4 μg of DNA/well; Promega, Madison, WI), was co-transfected to correct for transfection efficiency. Transfections were performed using Lipofectamine Plus Reagent (Life Technologies, Rockville, MD) according to the manufacturer's recommendations. Four hours after transfection, the medium was replaced with fresh medium in the absence of serum. Twenty-four hours after transfection, cells were either treated with AngII (10^{-7} M) or left untreated, and 6 h later, cell extracts were prepared using a reporter lysis reagent (Promega). Aliquots of cell lysate were analyzed for CAT activity after normalization for protein content or β-galactosidase activity as described previously (9).

Chromatin Immunoprecipitation

Chromatin immunoprecipitation (ChIP) assays were performed using reagents and protocols from Upstate Biotechnology as described previously (10,30). IMCD3 cells were plated in 10-cm culture dishes and starved for 24 h before AngII treatment. After AngII stimulation (10^{-7} M) for the indicated time periods, cells were incubated with 1% formaldehyde solution in growth medium for cross-linking (10 min at room temperature) followed by addition of 1 ml of 10× glycine to quench unreacted formaldehyde for 5 min at room temperature. Cell pellets were resuspended in SDS lysis buffer that contained protease inhibitor and phosphatase inhibitor cocktails. DNA was sheared by sonicating the cell lysate to produce an average DNA fragment size between 200 and 1000 bp and diluted 10-fold in ChIP dilution buffer. Immunoprecipitation was performed with antibodies to p-CREB (Ser133; Upstate Biotechnology; 06-519; 20 μl), CREB-1 (Santa Cruz; 240, sc-58; 25 μl), acetylated H4 (Upstate Cell Signaling; 06-866; 1:150 dilution), or control normal Ig (IgG) antibodies overnight at 4°C. DNA-protein-antibody complexes were captured on protein A/G-conjugated agarose beads. DNA-protein cross-links were reversed at 65°C overnight followed by proteinase K treatment to free DNA. Immunoprecipitated DNA was purified by spin column and subjected to PCR. Sequences of the primers that were used for PCR of the mouse B2R gene that flanked the p53-CRE enhancer are as follows: Forward primer 5′-AGG GGG GAG GTG CCC AGG AGA GTG ATG ACA-3′; reverse primer 5′-GGT TCT GTG TTG TAG GGA GT-3′.

Statistical Analyses

All data are expressed as means ± SEM and analyzed by *t* test or one-way ANOVA. All experiments were performed at least three times in duplicate. Differences between experimental groups were considered statistically significant at $P < 0.05$.

Results

AngII Upregulates BdkrB2 Gene Expression in Renal Collecting Duct Cells

Previous studies suggested the presence of AT_1R and B2R in several renal cell types, including vascular (smooth muscle, juxtaglomerular, endothelial) and collecting duct cells (31,32). Using double-immunofluorescence staining, we show that AT_1R and B2R are coexpressed on the cell membrane of mouse IMCD3 cells (Figure 1A). Control experiments that were conducted in the absence of primary antibodies revealed no specific staining (data not shown). AngII signals *via* two receptors, AT_1R and AT_2R, which are coupled to different intracellular signaling pathways. Reverse transcriptase–PCR (RT-PCR) assays were therefore performed to determine the AngII receptor type(s) expressed by IMCD3 cells. The results revealed that

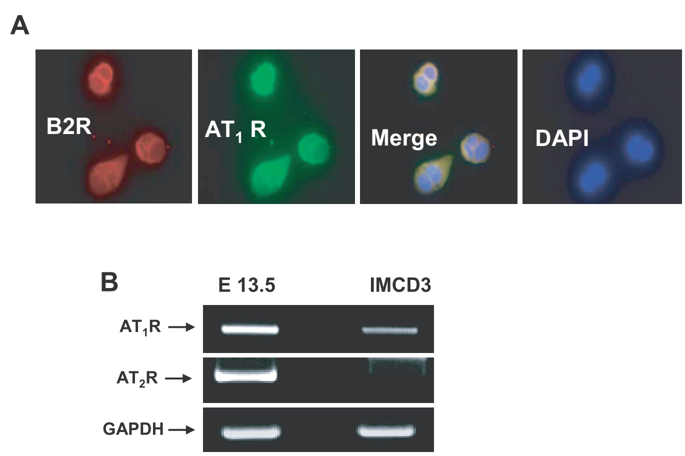

Figure 1. Expression of bradykinin (B2R) and angiotensin II (AngII) type 1 receptor (AT_1R) in inner medullary collecting duct (IMCD3) cells. (A) Immunofluorescence staining of B2R (red) and AT_1R (green) in IMCD3 cells. Merged images (yellow) suggest that IMCD3 cells coexpress AT_1 and B2R protein. (B) Reverse transcriptase–PCR (RT-PCR) showing expression of AT_1R mRNA in IMCD3 cells. In contrast, there is little if any expression of AT_2R mRNA in these cells. RNA from embryonic mouse kidneys (E13.5) was used as a positive control, and glyceraldehyde-3-phosphate dehydrogenase (GAPDH) was used as a loading control. Magnification, ×100.

IMCD3 cells express predominantly AT_1R transcripts; in contrast, only minimal amounts of AT_2R mRNA were detectable (Figure 1B). Positive control RNA samples from E13.5 mouse embryonic kidneys showed abundant AT_1R and AT_2R transcripts. These results indicate that IMCD3 cells express predominantly the AT_1R.

To test whether AngII regulates *BdkrB2* gene expression, we stimulated quiescent IMCD3 cells with AngII (10^{-7} M), in the presence or absence of the AT_1R antagonist candesartan (10^{-6} M). Total cellular RNA was extracted 3 or 24 h later. Untreated cells served as controls. RT-PCR showed a significant increase in *BdkrB2* mRNA levels in AngII-treated as compared with controls (190% at 3 h and 70% at 24 h; $P < 0.05$; Figure 2). Candesartan abrogated the stimulatory effect of AngII on *BdkrB2* gene expression, indicating that the AngII-induced increase in *BdkrB2* mRNA is mediated by the AT_1R (Figure 2).

Next, we investigated whether AngII upregulates B2R gene expression at the protein level. Quiescent IMCD3 cells were treated with varying concentrations of AngII (10^{-10} to 10^{-6} M), whereas untreated cells were used as control. Whole-cell lysates were collected 8, 24, and 48 h after AngII treatment and subjected to Western blot analysis. As shown in Figure 3, AngII stimulated dosage-dependent increases in B2R protein expression as early as 8 h after treatment and persisted for up to 48 h (8 h 2.6 ± 0.3-fold; 24 h 2.9 ± 0.4-fold; 48 h 2.2 ± 0.3-fold relative to control; $P < 0.05$ *versus* control). Collectively, these results demonstrate that AngII stimulates *BdkrB2* gene expression in IMCD3 cells at mRNA and protein levels.

AngII-Stimulated BdkrB2 Is Actinomycin D Sensitive

To explore the molecular mechanisms by which AngII regulates B2R gene expression, we pretreated quiescent IMCD3 cells with the transcriptional inhibitor actinomycin D (10^{-6} M) for 2 h, followed by AngII (10^{-7} M) for 6 h. Untreated cells were used as a control. Actinomycin D (10^{-6} M) abrogated the increase of *BdkrB2* mRNA levels induced by AngII (AngII 3.0 ± 0.69; AngII+actinomycin 0.45 ± 0.17 *versus* control; $P < 0.05$; $n = 4$; Figure 4A). These data suggest that AngII upregulates B2R gene expression at the transcriptional level.

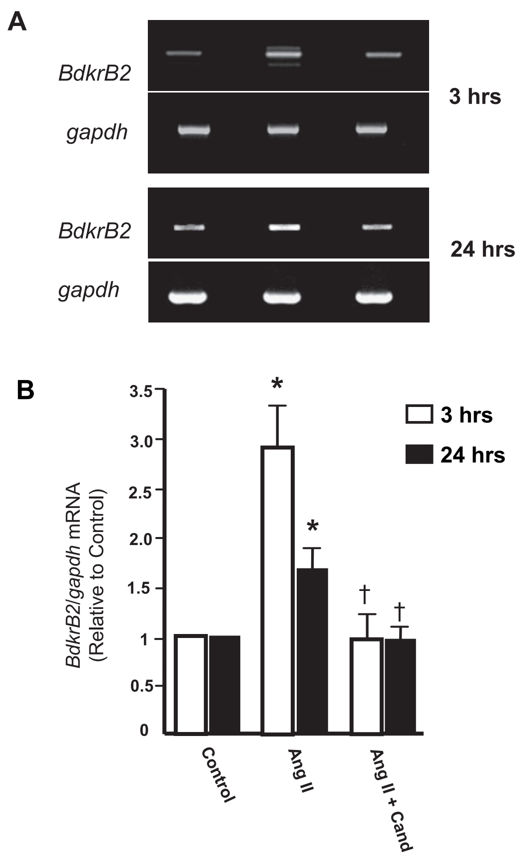

Figure 2. AngII upregulates *BdkrB2* gene expression. Quiescent IMCD3 cells were treated with AngII (10^{-7} M) in the absence or presence of the AT_1R antagonist candesartan (Cand; 10^{-6} M). Untreated cells served as time control. Total RNA was extracted 3 or 24 h after treatment, and RT-PCR was performed using mouse-specific *BdkrB2* and *gapdh* primers. (A) Ethidium bromide–stained gel. (B) Bar graph representing the means ± SEM of the ratios of *BdkrB2* and *gapdh* band intensities expressed relative to control. $^*P < 0.05$ *versus* other groups ($n = 3$); $^{\dagger}P < 0.05$ *versus* AngII.

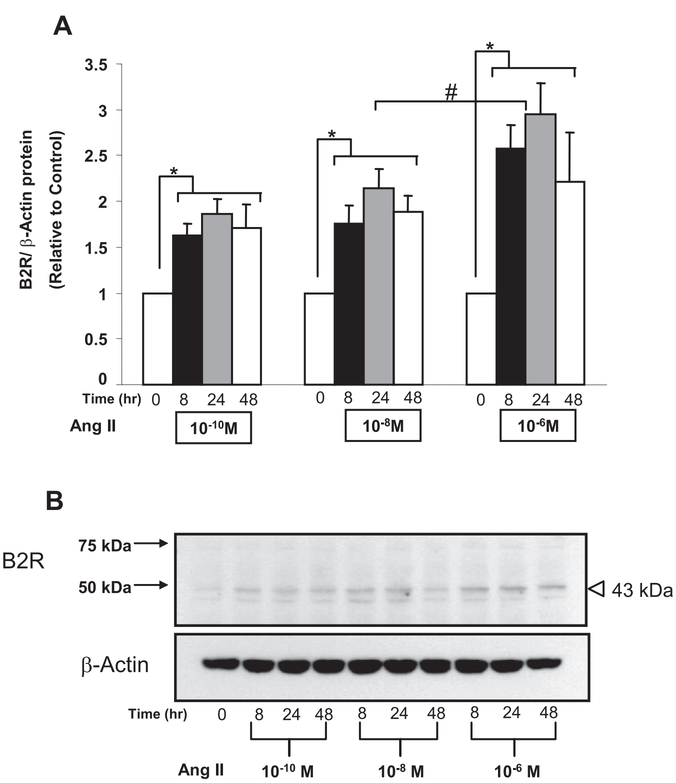

Figure 3. AngII upregulates B2R protein expression. Quiescent IMCD3 cells were treated with increasing concentrations of AngII (10^{-10} to 10^{-6} M). Untreated cells served as control. Whole-cell lysate was collected 8, 24, and 48 h after AngII treatment and was subjected to Western blot analysis. (A) Bar graph representing the ratios of B2R/β-actin band intensity expressed relative to control. (B) Immunoblots using anti-B2R and β-actin antibodies. B2R protein size is 43 kD. $^*P < 0.05$ *versus* control; $^{\#}P < 0.05$ *versus* 10^{-8} M AngII.

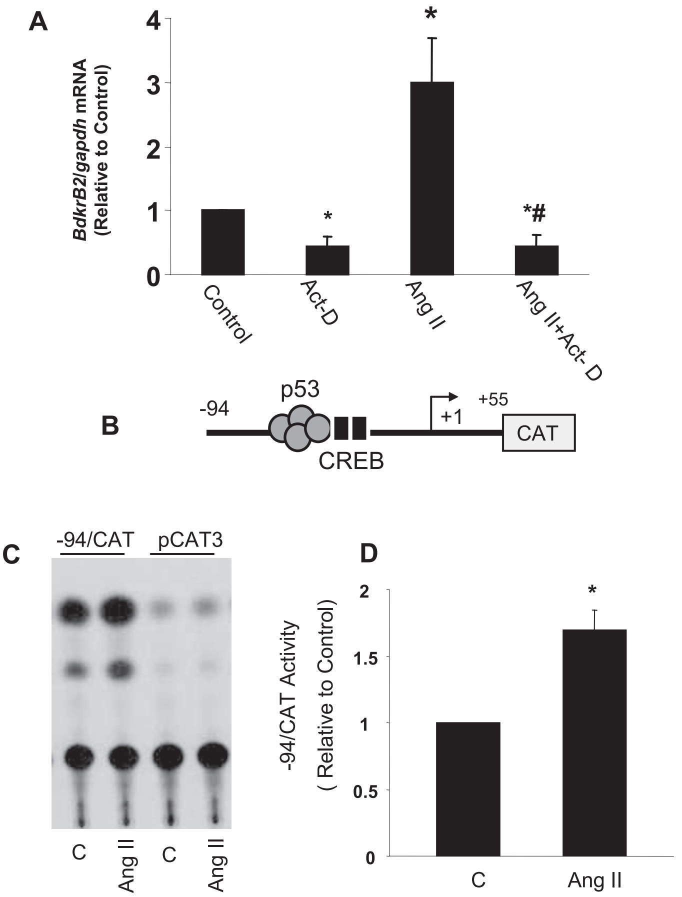

Figure 4. AngII stimulates *BdkrB2* gene transcription and promoter activity. (A) IMCD3 cells were treated with actinomycin D 2 h before addition of AngII or were treated with AngII alone. RNA was extracted 6 h after addition of AngII (10^{-7} M). RT-PCR was performed with mouse *BdkrB2* and *gapdh* primers. Bar graph represents the means ± SEM of the ratios of *BdkrB2/gapdh* band intensity expressed relative to control. **P* < 0.05 *versus* control (*n* = 4); #*P* < 0.05 *versus* AngII. (B) Schematic of *Bdkrb2* proximal promoter region, which contains a positive cis-acting enhancer composed of contiguous *cis*-binding sites for the transcription factors p53 and cAMP response element binding protein (CREB; nucleotides −44 to −69 relative to the transcription start site) (10). (C) Functional analysis of the effects of AngII on *BdkrB2* promoter activity. *BdkrB2* promoter-CAT construct (−94/CAT) or pCAT3Basic vector were transfected into IMCD3 cells. A control β-galactosidase vector, pSVZ, was co-transfected to correct for transfection efficiency. Twenty-four hours after transfection, cells were treated with AngII (10^{-7} M) for 6 h and cell lysate was assayed for CAT activity; untreated cells served as control. Bar graph represents the mean ± SEM of CAT activity expressed relative to control (untreated). **P* < 0.05 *versus* control (*n* = 5).

AngII Stimulates BdkrB2 Promoter Activity

In previous studies, we demonstrated that a highly conserved *BdkrB2* promoter fragment that extends from −94 to +55 bp, relative to the transcription start site at +1, is sufficient to drive reporter CAT activity in IMCD3 cells (10). This promoter region contains a composite cis-regulatory module for the transcription factors p53 and CREB, and cooperative interaction between the two proteins is essential for optimal *BdkrB2* promoter activity (10). Accordingly, we tested the effects of AngII on the activity of *BdkrB2* −94/+55-CAT promoter activity using transient transfection assays in IMCD3 cells (Figure 4B). The promoterless vector pCAT3Basic served as a control. Twenty-four hours after transfection, cells were treated with AngII (10^{-7} M) for 6 h and whole-cell lysates were harvested and assayed for CAT activity. As shown in Figure 4, C and D, AngII stimulated *BdkrB2* promoter-driven reporter activity to 1.7 ± 0.08-fold ($P < 0.05$ *versus* untreated cells; $n = 5$), whereas the promoterless construct pCAT3Basic was not affected by AngII.

To determine the functional importance of p53 and CREB in AngII-mediated transcriptional activation, we introduced mutations in the −94/+55-CAT construct at the p53(P1)- and CRE *cis*-regulatory elements, either singly or in combination. These mutations have been shown to inhibit the binding of p53 and CREB to their respective sites (10). IMCD3 cells were transiently transfected with −94/+55-CAT construct, the single-mutant constructs −94P1mut/CAT and −94CREmut/CAT, and the double mutant construct −94P1mutCREmut/CAT. Twenty-four hours after transfection, the cells were treated with AngII (10^{-7} M) for 6 h. CAT assays revealed that mutations in CRE or p53 binding sites, either singly or in combination, abrogated AngII-stimulated *BdkrB2* promoter activity (Figure 5).

AngII Stimulates CREB Phosphorylation and Association with BdkrB2 Promoter

Multiple signal transduction pathways are known to converge on the transcription factor CREB, leading to its phosphorylation on serine 133 (33). This posttranslational modification promotes the interaction of CREB with its co-activator, CBP/p300, and enhances CREB transcriptional activity (11,13). In addition, CREB phosphorylation has been shown to facilitate the interaction of CREB with p53 and thus their co-recruitments to target promoters (15,33). For examination of the effect of AngII on CREB phosphorylation, IMCD3 cells were incubated with AngII (10^{-7} M) and cellular lysates were harvested at various time points ranging from 0 to 60 min. The lysate was subjected to Western blotting using p-ser133-CREB or CREB antibodies. The results showed that AngII significantly increased p-CREB/CREB ratio at 30 min after stimulation (Figure 6, A and B).

We next asked whether AngII stimulation promotes the binding of p-CREB to the endogenous *BdkrB2* promoter using ChIP-PCR. As shown in Figure 6C, baseline occupancy of *BdkrB2* promoter by p-CREB was minimal and comparable to background levels. This was not due to the lack of CREB binding to the promoter (Figure 6C). Exposure of IMCD3 cells to AngII for 15 min induced a considerable increase in p-CREB at the *BdkrB2* promoter to 3.3-fold ($n = 2$) relative to control. Consistent with the ability of p-CREB to interact with and recruit CBP/p300, this effect was associated with hyperacetylation of promoter-associated histone H4 (Figure 6D). These results indicate that AngII stimulates association of p-CREB with the *BdkrB2* pro-

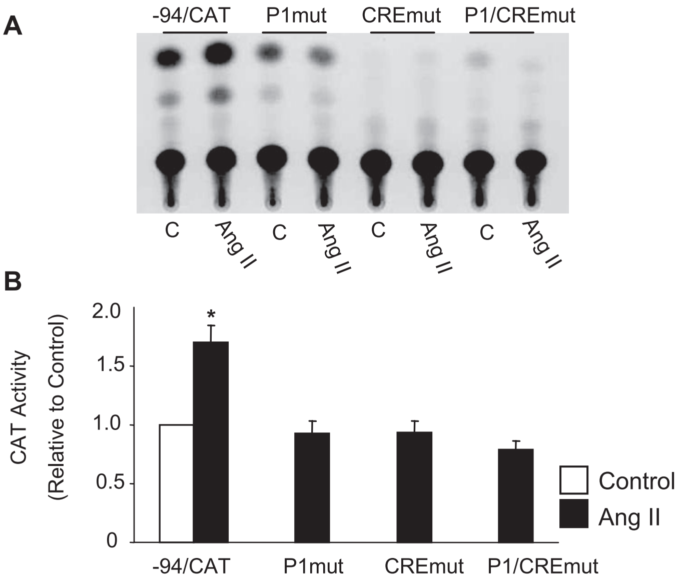

Figure 5. AngII activates the *BdkrB2* promoter *via* the p53-CRE module. (A) CAT assay. Site-directed mutagenesis was used to introduce mutations in the −94/+55-CAT construct at the p53(P1)- and CRE-response elements, singly or in combination. The wild-type −94/+55-CAT, −94P1mut/CAT (mutant p53-binding site), −94CREmut/CAT (mutant CREB binding site), or −94P1mut.CREmut/CAT (double mutant) constructs were transfected into IMCD3 cells. Twenty-four hours after transfection, cells were treated with AngII (10^{-7} M) for 6 h and cell lysate was subjected to CAT activity assay as described in Figure 4. A control β-galactosidase vector, pSVZ, was co-transfected to correct for transfection efficiency. Twenty-four hours after transfection, cells were treated with AngII (10^{-7} M) for 6 h and cell lysate was subjected to CAT activity assay after normalization for β-galactosidase activity; untreated cells as control. (B) Bar graph represents the mean ± SEM of CAT activity expressed relative to control (untreated). $^*P < 0.05$ *versus* −94/CAT control ($n = 5$).

moter and localized promoter hyperacetylation, an epigenetic marker of transcriptional activation.

AngII-Treated Cells Exhibit Enhanced Intracellular B2R-Ca^{2+} Signaling

To determine whether AngII-mediated induction of *BdkrB2* gene expression is accompanied by a functional cellular response, we evaluated the effect of 24-h AngII treatment on BK-induced intracellular calcium $[Ca^{2+}]_i$ in IMCD3 cells. Figure 7A shows that the mean peak responses to BK (10^{-9} and 10^{-7} M) were Δ23.4 ± 3.9 nM and Δ46.8 ± 9.03 nM ($n = 8$ and 6, respectively; $P < 0.05$) above baseline. This finding confirms that B2R is coupled to intracellular Ca^{2+} signaling in IMCD3 cells. For testing the effect of AngII on B2R signaling, the cells were treated with AngII (10^{-7} M) for 24 h before exposure to BK (10^{-7} M). Untreated cells were used as a control. Figure 7B shows that the mean peak response to BK in AngII-treated cells was 87.12 ± 12.45 nM above baseline, compared with 39.20 ± 4.61 nM in untreated cells ($n = 14$ and 15, respectively; $P < 0.05$). The B2R antagonist icatibant (10^{-6} M) reduced the mean peak response to BK to 16.10 ± 2.59 nM in AngII-treated cells ($n = 10$; $P < 0.05$; Figure 7B). The results indicate that AngII-treated cells respond by increasing B2R mRNA and protein synthesis as well as by enhanced membrane-associated B2R signaling.

Reduced BdkrB2 Gene Expression in $Agtr1_A$-Null Mice

To determine whether the *BdkrB2* gene is regulated by AngII *in vivo*, we compared *BdkrB2* mRNA levels in wild-type *versus* $Agtr1_A{}^{-/-}$, $Agtr1_B{}^{-/-}$, or $Agtr1_A{}^{-/-}{}_{/B}{}^{-/-}$ mice. RT-PCR revealed that *BdkrB2* mRNA levels, factored for GAPDH, were 53% lower in the renal medulla of $Agtr1_A{}^{-/-}$ and $Agtr1_{A/B}{}^{-/-}$ than in $Agtr1^{+/+}$ and $Agtr1_B{}^{-/-}$ mice (0.14 ± 0.01 *versus* 0.3 ± 0.06 units; $P < 0.05$; Figure 8A). In contrast, the renal cortex showed no differences in *BdkrB2* gene expression among the genotypes (data not shown). *BdkrB2* mRNA levels tended to be lower in the heart of $Agtr1_A{}^{-/-}$ and $Agtr1_A{}^{-/-}/_B{}^{-/-}$ than in $Agtr1^{+/+}$ and $Agtr1_{1B}{}^{-/-}$ mice (0.54 ± 0.04 *versus* 0.64 ± 0.02; factored for GAPDH; $P = 0.07$; Figure 8B). These results together with the cell culture data support the notion that *BdkrB2* gene expression is under physiologic regulation by AngII.

Discussion

AngII, acting *via* AT_1R, stimulates renal tubular sodium and water reabsorption and causes renal vasoconstriction. In contrast, kinins promote natriuresis and diuresis and increase renal blood flow *via* stimulation of B2R. Therefore, the balance between the RAS and KKS affects salt and water handling, volume homeostasis, and BP control (2). This is well illustrated in $BdkrB2^{-/-}$ mice, which are susceptible to AngII-induced hypertension (22). AT_1R and B2R belong to the seven-transmembrane GPCR family of receptors and are coexpressed in several cell types, including vascular and renal epithelial cells, including the renal collecting duct (31,32). Both short- and long-loop interactive pathways exist between the AT_1R and B2R. In the short-loop pathway, AT_1R and B2R communicate directly with each other. The two receptors form stable heterodimers, resulting in enhanced activation of AT_1R signaling (4). The AT_1R–B2R complex seems to signal as a "super AT_1R." It is interesting that a significant increase in AT_1R–B2R heterodimerization occurs in hypertensive preeclamptic women and is associated with a five-fold upregulation in B2R levels (5). Our findings in this study support the concept that *BdkrB2* gene expression is positively regulated by AngII and that signaling *via* AT_1R–B2R activates B2R expression.

The long-loop pathway that connects AT_1R and B2R receptors involves gene regulation. This cross-regulatory pathway seems to operate in cardiac/vascular smooth muscle cells and, as shown in this study, in renal collecting duct cells. Infusion of subpressor doses of AngII into wild-type mice upregulates cardiac myocyte *BdkrB2* mRNA by 47% (6). Furthermore, treatment of vascular smooth muscle cells in culture with AngII produces a time-dependent induction of *BdkrB2* mRNA that is maximal at 3 h and declines to baseline by 24 h. This effect is blocked by AT_1R antagonism (6). This study provides new evidence that the *BdkrB2* gene is a downstream target of the $AT_{1A}R$ *in vivo*. This conclusion is based on the following find-

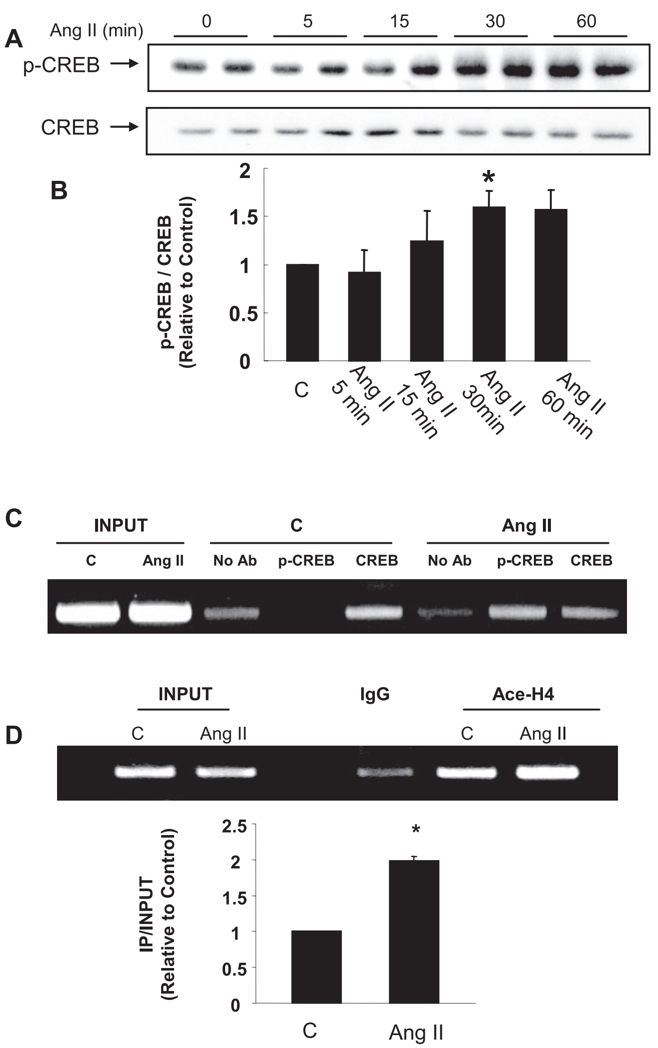

Figure 6. AngII stimulates CREB phosphorylation, p-CREB occupancy of *BdkrB2* promoter, and histone hyperacetylation. (A) Western blot analysis. IMCD3 cells were stimulated with AngII (10^{-7} M), and cell lysates were collected at the indicated time points. Immunoblots were probed with antibodies to CREB or Ser-133 p-CREB. (B) Densitometric analysis of ratios of p-CREB/CREB band densities expressed relative to control. $^*P < 0.05$ *versus* untreated and AngII 5-min samples. (C) Chromatin immunoprecipitation (ChIP) assay of the *BdkrB2* promoter in AngII-treated IMCD3 cells using anti-CREB and anti–p-CREB (ser133) antibodies. PCR amplification of the immunoprecipitated genomic DNA was performed using primers that flank the p53-CRE module. In unstimulated cells, the *BdkrB2* promoter is occupied by CREB, whereas the p-CREB signal is minimal. After AngII stimulation (10^{-7} M, 15 min), p-CREB occupancy of the promoter is enhanced, whereas the total CREB signal remains unchanged (n = 2 independent experiments). (D) ChIP assay of the *BdkrB2* promoter in AngII-treated IMCD3 cells using anti-acetylated histone (Ace-H4) antibody or nonspecific IgG (control). PCR amplification of the immunoprecipitated genomic DNA was performed using primers that flank the p53-CRE module. PCR amplification of the immunoprecipitated genomic DNA revealed enrichment of Ace-H4 in AngII-treated cells 2 h after AngII stimulation as compared with untreated samples (n = 3). Similar results were obtained at 4 and 6 h (data not shown). (E) Quantitative analysis of Ace-H4 enrichment on *BdkrB2* promoter expressed relative to input DNA. $^*P < 0.05$ *versus* control.

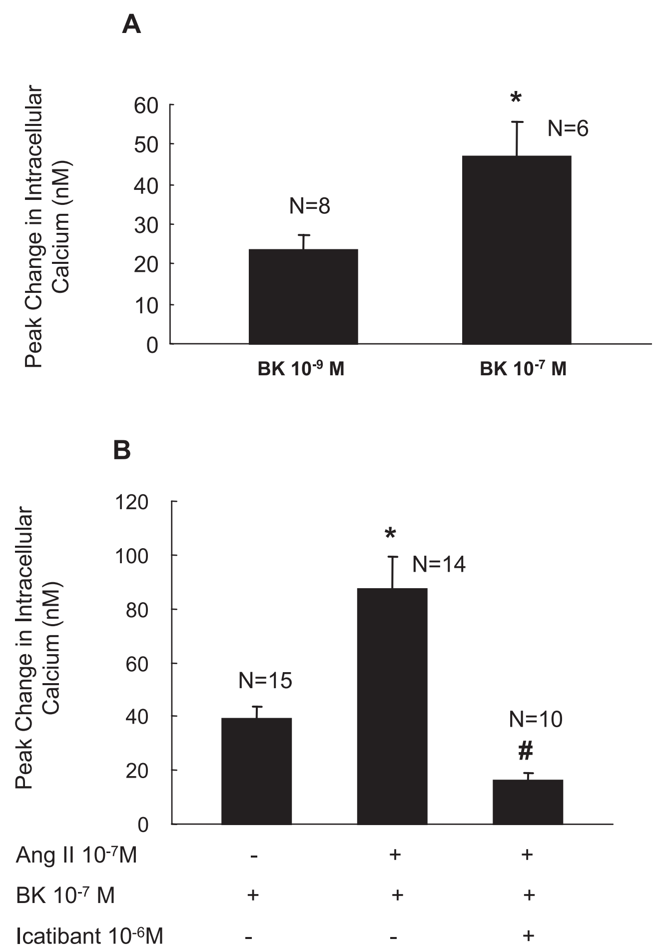

Figure 7. AngII stimulates B2R calcium signaling. (A) Bar graph depicts increases in intracellular [Ca^{2+}] in response to BK stimulation in IMCD3 cells relative to baseline levels (absolute baseline levels are 43.7 ± 7.8 nM). $^*P < 0.05$ *versus* BK 10^{-9} M. (B) Bar graph shows the intracellular Ca^{2+} response to BK in IMCD3 cells that were treated with AngII for 24 h before exposure to BK in the absence or presence of the B2R competitive antagonist icatibant. Untreated cells served as a control. $^*P < 0.05$ *versus* BK alone; $^{\#}P < 0.001$ *versus* AngII 10^{-7} M + BK 10^{-7} M.

ings: (*1*) *Agtr1*$_A^{-/-}$ or *Agtr1*$_A^{-/-}$/$_B^{-/-}$ mice have reduced levels of *BdkrB2* mRNA in the renal medulla as compared with wild-type or *Agtr1*$_B^{-/-}$ mice; (*2*) exogenous AngII upregulates *BdkrB2* mRNA and protein expression in IMCD3 cells, and this effect can be blocked by AT_1R blocker; (*3*) AngII stimulates *BdkrB2* gene transcription and promoter-driven reporter activity; (*4*) AngII promotes occupancy of the *BdkrB2* promoter by activated CREB; and (*5*) AngII-treated cells exhibit augmented B2R-mediated intracellular calcium signaling in response to acute bradykinin stimulation. The AT_1R–B2R feed-forward mechanism creates a new level of cross-talk between two GPCR with wide-ranging implications on renal salt and water handling, BP regulation, and growth and differentiation.

In the kidney, AT_1R and B2R are expressed in a developmentally regulated manner, increasing from relatively low levels in the embryo to peak levels perinatally (34). Moreover, immuno-

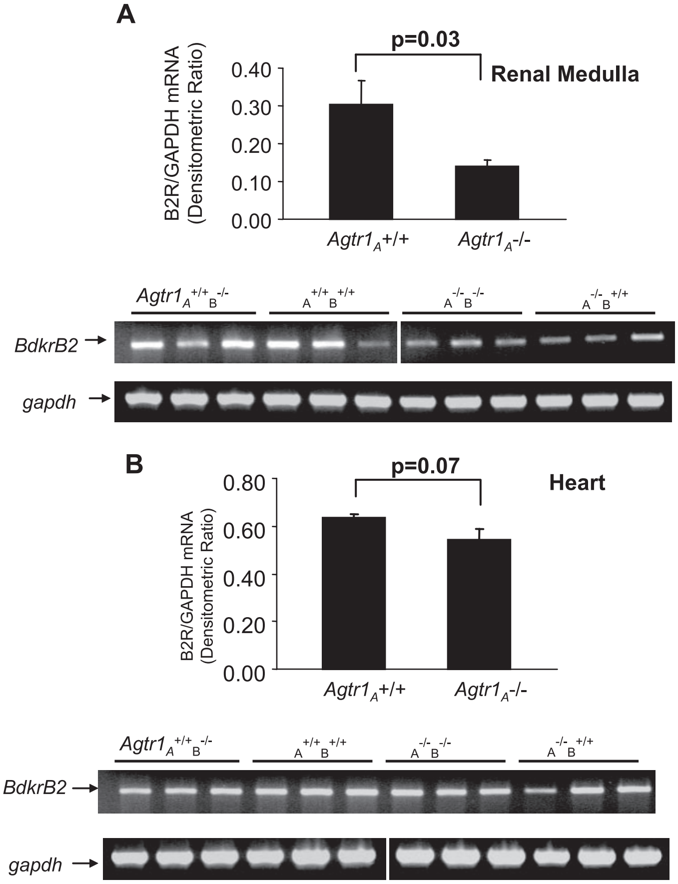

Figure 8. Reduced renal *BdkrB2* gene expression in *Agtr1$_A$* knockout mice. Total RNA from renal medulla (A) or heart (B) of *Agtr1$_A$$^{+/+}$* and *Agtr1$_A$$^{-/-}$* mice was subjected to RT-PCR using mouse *BdkrB2* and *gapdh* primers as described in Materials and Methods. Bar graphs represent the mean ± SEM of *BdkrB2/gapdh* band intensity (n = 3 per genotype). $^*P < 0.05$ *versus Agtr1$^{+/+}$*.

histochemical analysis has shown that AT$_1$R are more widely distributed along the nephron than previously recognized, including renal vascular smooth muscle and proximal and distal epithelial sites (31). B2R is expressed primarily in collecting duct cells but also in the vascular and interstitial elements within the kidney (26,32). In rodents, there are two subtypes of AT$_1$R: AT$_{1A}$ and AT$_{1B}$. AT$_{1A}$ is the predominant subtype expressed in most tissues and mediates the known physiologic functions of AngII. This study demonstrated that *BdkrB2* mRNA levels were 53% lower in the renal medulla of *Agtr1$_A$$^{-/-}$* than in *Agtr1$^{+/+}$* or *Agtr1$_B$$^{-/-}$* mice. In contrast, the renal cortex showed no differences, indicating that renal medullary *BdkrB2* gene expression is regulated by AngII *via* the AT$_{1A}$R subtype. This study also showed that cardiac *BdkrB2* mRNA levels tended to be lower in *Agtr*1$_A$$^{-/-}$ than in *Agtr*1$_A$$^{+/+}$ mice, consistent with previous data showing that AngII induces *BdkrB2* gene expression in cardiac myocytes and vascular smooth muscle cells (6,7). It is important to note here that because our studies were performed in adult mouse kidneys and IMCD cells, in which AT$_{1A}$ is the predominant AngII receptor, it is not surprising that AngII effects were mediated by AT$_{1A}$, rather than AT$_{1B}$ or AT2. These findings do not, however, preclude similar interactions between these receptors and B2R in relevant tissues (adrenal, AT$_{1B}$) or developmental stages (embryos, AT2).

IMCD3 cells are epithelial cells that retain many differentiated characteristics of the inner medullary collecting duct *in vivo* (20). As shown in this study, IMCD3 cells express AT$_1$R and B2R mRNA and protein, whereas AT$_2$R mRNA was difficult to detect. Therefore, IMCD3 cells express predominantly the AT$_1$R subtype, which is compatible with the finding that AngII-induced B2R gene expression was completely abrogated by pharmacologic AT$_1$R antagonism. As a GPCR, B2R generally signals through Gα_q to stimulate phospholipase C$_\beta$. In addition, B2R interacts with several other G proteins, including Gα_i, Gα_s, and G$\alpha_{12/13}$. BK stimulates Gα_q-sensitive phospholipase C$_\beta$, leading to phosphoinositide hydrolysis and intracellular free Ca^{2+} mobilization. Increased intracellular Ca^{2+} can in turn mediate the activation of cytosolic Ca^{2+}-dependent endothelium nitric oxide synthase and Ca^{2+}-sensitive phospholipase A2, thereby leading to nitric oxide and prostaglandin release (35). Our study showed that AngII treatment amplifies the intracellular Ca^{2+} response to bradykinin, whereas the B2R antagonist icatibant reduces the peak response to bradykinin in AngII-treated cells. Altogether, these data indicate that AngII stimulates B2R signaling in renal epithelial cells.

The *BdkrB2* gene is located on human chromosome 14, mouse chromosome 12, and rat chromosome 6. The overall organization and structure of the *BdkrB2* gene are generally similar in the three species: Three exons and two introns. The human and the rat but not the murine *BdkrB2* genes have an alternatively spliced exon between exons 2 and 3, termed exon 2b. The coding sequence of *BdkrB2* resides in exon 3 (36,37). Previous analysis of the rat *BdkrB2* gene identified a modular enhancer located at nucleotides −44 to −82 of rat *BdkrB2* promoter, which is 100% conserved between rat and mouse and 85% conserved between rat and human genes (10). The *BdkrB2* enhancer receives inputs from three transcription factors with overlapping expression in the collecting ducts, namely, p53, CREB, and KLF-4 (10). CREB phosphorylation on Ser-133 is required for optimal stimulation of *BdkrB2* promoter activity through recruitment of CBP and enhancement of p53–CREB interactions. Therefore, the renal collecting duct epithelial cells contain the necessary machinery for the regulation of *BdkrB2* transcription. The sequence similarities between rodent and human proximal BdkrB2 promoter regions suggest that these control factors exist in the human kidney.

This study demonstrates that AngII-induced *BdkrB2* gene expression is mediated transcriptionally because it is completely blocked by actinomycin D. Moreover, a promoter–reporter construct that harbors the modular *BdkrB2* enhancer is responsive to AngII stimulation. Our investigations of the signaling inputs that link the AT$_1$R to the *BdkrB2* enhancer revealed several important findings. First, AngII stimulates the phosphorylation of CREB on Ser-133 within 15 to 30 min, a modification that is required for the interaction of CREB with its co-activator, CBP/p300, resulting in enhanced CREB transcriptional activity (11). Second, as demonstrated by ChIP, AngII stimulated occupancy of the *BdkrB2* promoter by activated CREB, as well as induced promoter histone hyperacetylation. These events also occurred within 30 min. Acetylation of promoter-associated nucleosomes is thought to relax the chromatin structure, thereby facilitating access of transcriptional activators to their binding sites on DNA (38). Third, introduction of point mutations in the CRE- or p53-binding sites abrogated AngII-induced activation of the *BdkrB2* promoter. Fourth, RT-PCR analysis revealed upregulated expression of *BdkrB2* mRNA as early as 3 h after stimulation with AngII. On the basis of these findings, we propose a model in which AT_1R signaling stimulates sequential series of events that lead to phosphorylation of CREB and its binding to the p53-CRE modular enhancer in the *BdkrB2* promoter. Phosphorylation of CREB promotes recruitment of CBP and p53 and stimulates localized histone hyperacetylation and activation of *BdkrB2* transcription in renal epithelial cells. The enhanced transcription of *BdkrB2* gene leads to augmented mRNA and protein levels, which results in enhanced intracellular calcium signaling and functional responses to bradykinin.

Acknowledgments

Support for this study was provided by grants from the National Institutes of Health DK-56264, DK-62250, DK-62003, and P20RR017659; a predoctoral fellowship grant from the American Heart Association; the Tulane Hypertension and Renal Center of Excellence; and Louisiana Board of Regents, through the Millennium Trust Health Excellence Fund.

Disclosures

None.

References

1. Tschope C, Schultheiss HP, Walther T: Multiple interactions between the renin-angiotensin and the kallikrein-kinin systems: Role of ACE inhibition and AT1 receptor blockade. *J Cardiovasc Pharmacol* 39: 478–487, 2002
2. Schmaier AH: The kallikrein-kinin and the renin-angiotensin systems have a multilayered interaction. *Am J Physiol Regul Integr Comp Physiol* 285: R1–R13, 2003
3. Shen B, El-Dahr SS: Cross-talk of the renin-angiotensin and kallikrein-kinin systems. *Biol Chem* 387: 145–150, 2006
4. AbdAlla S, Lother H, Quitterer U: AT1-receptor heterodimers show enhanced G-protein activation and altered receptor sequestration. *Nature* 407: 94–98, 2000
5. AbdAlla S, Lother H, el Massiery A, Quitterer U: Increased AT(1) receptor heterodimers in preeclampsia mediate enhanced angiotensin II responsiveness. *Nat Med* 7: 1003–1009, 2001
6. Kintsurashvili E, Duka I, Gavras I, Johns C, Farmakiotis D, Gavras H: Effects of ANG II on bradykinin receptor gene expression in cardiomyocytes and vascular smooth muscle cells. *Am J Physiol Heart Circ Physiol* 281: H1778–H1783, 2001
7. Tan Y, Hutchison FN, Jaffa AA: Mechanisms of angiotensin II-induced expression of B2 kinin receptors. *Am J Physiol Heart Circ Physiol* 286: H926–932, 2004
8. Marks J, Saifudeen Z, Dipp S, El-Dahr SS: Two functionally divergent p53-responsive elements in the rat bradykinin B2 receptor promoter. *J Biol Chem* 278: 34158–34166, 2003
9. Saifudeen Z, Du H, Dipp S, El-Dahr SS: The bradykinin type 2 receptor is a target for p53-mediated transcriptional activation. *J Biol Chem* 275: 15557–15562, 2000
10. Saifudeen Z, Dipp S, Fan H, El-Dahr SS: Combinatorial control of the bradykinin B2 receptor promoter by p53, CREB, KLF-4, and CBP: Implications for terminal nephron differentiation. *Am J Physiol Renal Physiol* 288: F899–F909, 2005
11. Cardinaux JR, Notis JC, Zhang Q, Vo N, Craig JC, Fass DM, Brennan RG, Goodman RH: Recruitment of CREB binding protein is sufficient for CREB-mediated gene activation. *Mol Cell Biol* 20: 1546–1552, 2000
12. An W, Palhan VB, Karymov MA, Leuba SH, Roeder RG: Selective requirements for histone H3 and H4 N termini in p300-dependent transcriptional activation from chromatin. *Mol Cell* 9: 811–821, 2002
13. Yuan LW, Gambee JE: Histone acetylation by p300 is involved in CREB-mediated transcription on chromatin. *Biochim Biophys Acta* 1541: 161–169, 2001
14. Legube G, Trouche D: Regulating histone acetyltransferases and deacetylases. *EMBO Rep* 4: 944–947, 2003
15. Giebler HA, Lemasson I, Nyborg JK: p53 recruitment of CREB binding protein mediated through phosphorylated CREB: A novel pathway of tumor suppressor regulation. *Mol Cell Biol* 20: 4849–4858, 2000
16. Leri A, Claudio PP, Li Q, Wang X, Reiss K, Wang S, Malhotra A, Kajstura J, Anversa P: Stretch-mediated release of angiotensin II induces myocyte apoptosis by activating p53 that enhances the local renin-angiotensin system and decreases the Bcl-2-to-Bax protein ratio in the cell. *J Clin Invest* 101: 1326–1342, 1998
17. Pierzchalski P, Reiss K, Cheng W, Cirielli C, Kajstura J, Nitahara JA, Rizk M, Capogrossi MC, Anversa P: p53 induces myocyte apoptosis via the activation of the renin-angiotensin system. *Exp Cell Res* 234: 57–65, 1997
18. Funakoshi Y, Ichiki T, Takeda K, Tokuno T, Iino N, Takeshita A: Critical role of cAMP-response element-binding protein for angiotensin II-induced hypertrophy of vascular smooth muscle cells. *J Biol Chem* 277: 18710–18717, 2002
19. Harrison-Bernard LM, Monjure CJ, Bivona BJ: Efferent arterioles exclusively express the subtype 1A angiotensin receptor: Functional insights from genetic mouse models. *Am J Physiol Renal Physiol* 290: F1177–F1186, 2006
20. Rauchman MI, Nigam SK, Delpire E, Gullans SR: An osmotically tolerant inner medullary collecting duct cell line from an SV40 transgenic mouse. *Am J Physiol* 265: F416–F424, 1993
21. Cervenka L, Harrison-Bernard LM, Dipp S, Primrose G, Imig JD, El-Dahr SS: Early onset salt-sensitive hypertension in bradykinin B(2) receptor null mice. *Hypertension* 34: 176–180, 1999
22. Cervenka L, Maly J, Karasova L, Simova M, Vitko S, Hellerova S, Heller J, El-Dahr SS: Angiotensin II-induced hypertension in bradykinin B2 receptor knockout mice. *Hypertension* 37: 967–973, 2001
23. El-Dahr SS, Dipp S, Baricos WH: Bradykinin stimulates the ERK–>Elk-1–>Fos/AP-1 pathway in mesangial cells. *Am J Physiol* 275: F343–F352, 1998

24. El-Dahr SS, Dipp S, Yosipiv IV, Baricos WH: Bradykinin stimulates c-fos expression, AP-1-DNA binding activity and proliferation of rat glomerular mesangial cells. *Kidney Int* 50: 1850–1855, 1996
25. El-Dahr SS, Yosipiv IV, Lewis L, Mitchell KD: Role of bradykinin B2 receptors in the developmental changes of renal hemodynamics in the neonatal rat. *Am J Physiol* 269: F786–F792, 1995
26. Figueroa CD, Gonzalez CB, Grigoriev S, Abd Alla SA, Haasemann M, Jarnagin K, Muller-Esterl W: Probing for the bradykinin B2 receptor in rat kidney by anti-peptide and anti-ligand antibodies. *J Histochem Cytochem* 43: 137–148, 1995
27. Iosipiv IV, Schroeder M: A role for angiotensin II AT1 receptors in ureteric bud cell branching. *Am J Physiol Renal Physiol* 285: F199–F207, 2003
28. Grynkiewicz G, Poenie M, Tsien RY: A new generation of Ca2+ indicators with greatly improved fluorescence properties. *J Biol Chem* 260: 3440–3450, 1985
29. Inscho EW, Mason MJ, Schroeder AC, Deichmann PC, Stiegler KD, Imig JD: Agonist-induced calcium regulation in freshly isolated renal microvascular smooth muscle cells. *J Am Soc Nephrol* 8: 569–579, 1997
30. Saifudeen Z, Diavolitsis V, Stefkova J, Dipp S, Fan H, El-Dahr SS: Spatiotemporal switch from DeltaNp73 to TAp73 isoforms during nephrogenesis: Impact on differentiation gene expression. *J Biol Chem* 280: 23094–23102, 2005
31. Harrison-Bernard LM, Navar LG, Ho MM, Vinson GP, El-Dahr SS: Immunohistochemical localization of ANG II AT1 receptor in adult rat kidney using a monoclonal antibody. *Am J Physiol* 273: F170–F177, 1997
32. El-Dahr SS, Figueroa CD, Gonzalez CB, Muller-Esterl W: Ontogeny of bradykinin B2 receptors in the rat kidney: Implications for segmental nephron maturation. *Kidney Int* 51: 739–749, 1997
33. Shaywitz AJ, Greenberg ME: CREB: A stimulus-induced transcription factor activated by a diverse array of extracellular signals. *Annu Rev Biochem* 68: 821–861, 1999
34. Norwood VF, Craig MR, Harris JM, Gomez RA: Differential expression of angiotensin II receptors during early renal morphogenesis. *Am J Physiol* 272: R662–R668, 1997
35. Leeb-Lundberg LM, Marceau F, Muller-Esterl W, Pettibone DJ, Zuraw BL: International union of pharmacology. XLV. Classification of the kinin receptor family: From molecular mechanisms to pathophysiological consequences. *Pharmacol Rev* 57: 27–77, 2005
36. Baptista HA, Avellar MC, Araujo RC, Pesquero JL, Schanstra JP, Bascands JL, Esteve JP, Paiva AC, Bader M, Pesquero JB: Transcriptional regulation of the rat bradykinin B2 receptor gene: Identification of a silencer element. *Mol Pharmacol* 62: 1344–1355, 2002
37. Kammerer S, Braun A, Arnold N, Roscher AA: The human bradykinin B2 receptor gene: Full length cDNA, genomic organization and identification of the regulatory region. *Biochem Biophys Res Commun* 211: 226–233, 1995
38. Berger SL: Histone modifications in transcriptional regulation. *Curr Opin Genet Dev* 12: 142–148, 2002